Charge-transfer devices and their application in physics

L. M. Soroko

Joint Institute for Nuclear Research, Dubna
Fiz. Elem. Chastits At. Yadra **10**, 1038–1074 (September–October 1979)

The physical properties and technical characteristics of charge-transfer devices are described. The use of these devices in image-scanning systems, memory devices, real-time spectral transformations, and in their first application to streamer chambers is described. The topological transformations which can be made with the help of charge-transfer devices in the scanning of track images are discussed.

PACS numbers: 29.40.Hy, 29.60.Ef, 29.80. – j

FOREWARD

Charge-transfer devices are a variety of semiconductor device prepared on a single crystal of silicon with extrinsic conduction. The majority charge carriers in an extrinsic semiconductor are either electrons, which produce n-type conduction, or holes, which correspond to p-type conduction. The charges of the majority carriers are opposite to those of the minority carriers. If the semiconductor has a high density of doping, its conductivity is called n^+ or p^+. The resistivity of such a semiconductor is less than that of a semiconductor with a low density of doping.

At the contact of two semiconductors with opposite conductivity, a semiconducting junction arises which has the properties of an electrical diode. If an inversely biased diode is operated at a small bias voltage, then the current through the diode in this mode is produced only by the minority carriers of the semiconductor and its magnitude is directly proportional to the concentration of minority carriers in the vicinity of the semiconductor junction. The combination of two semiconductor junctions with a narrow diffusion region has the property of an electrical triode and is called a transistor. In a field-effect transistor the controlling electrode is insulated from the semiconductor channel by a layer of silicon oxide. This electrode is called the gate. A field-effect transistor contains a source and also a drain in the form of two islands of n^+ conductivity in a single crystal of silicon with p-type conduction.

A triple-layer or multilayer structure of field-effect transistors of the metal-oxide-semiconductor (MOS) type has become the basis of a broad class of semiconductor devices which includes charge-transfer devices. The reason for this is that semiconductor devices of this structure can be prepared by modern planar technology with a high degree of complexity of the device.

A charge-transfer device (CTD) has the structure of a one-dimensional chain or a two-dimensional matrix, each element of which consists of a microcapacitor of the metal-oxide-semiconductor type. The feature of a CTD is that the signal charge arising in the region of the microcapacitor and dropping into a potential well can be shifted from one potential well to a neighboring one along the chain of microcapacitors, which serves the function of an analog shift register. The fast action and low energy consumption are important technical characteristics of such a register.

Charge-transfer devices are used in image-scanning systems, in immediate-access memories, in analog correlators, and in fact real-time systems for spectral analysis. Charge-transfer devices are of considerable interest for high-energy physics as image detectors and as two-dimensional signal converters. Stanford in 1977 used CTDs for the first time in photographing events in a two-meter streamer chamber. Experimental studies carried out at Seattle have shown that the sensitivity of CTDs as optical image detectors is about 20 times better than the best photographic emulsion used in streamer photography.

In this review we describe the physical properties of CTDs and their technical characteristics. We discuss the application of CTDs in image-detection systems, memory devices, real-time spectral-analysis systems, and streamer chambers, and we describe algorithms for topological transformations in the scanning of track images which can be achieved by means of CTSs.

1. PRINCIPLE OF OPERATION OF CHARGE-TRANSFER DEVICES

A charge-transfer device[1-4] consists of a one-dimensional chain or a two-dimensional matrix, each element of which is a miniature electrical capacitor of the metal-oxide-semiconductor type (Fig. 1). If a positive voltage pulse is applied to the metallic electrode of such a capacitor, then the majority charge carries of the p-type semiconductor are displaced from the surface layer and a potential well arises under the gate. In the potential well produced, the minority charge carriers of the semiconductor begin to accumulate. Several mechanisms for the appearance of charges in the potential well exist: injection of charges from the dif-

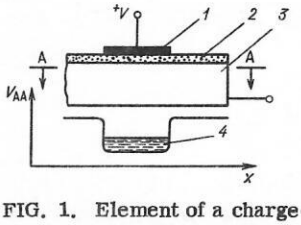

FIG. 1. Element of a charge-transfer device—a miniature electrical capacitor of the metal-oxide-semiconductor type: 1—metallic electrode, 2—dielectric, 3—p-type semiconductor, 4—shape of potential well formed near the surface separating the oxide and the semiconductor.

 0090-4759/79/050412-16$02.80

fusion region of the semiconductor, formation of charges on absorption of photons, and the thermal production process.[1] Under the influence of the charges accumulated in the potential well, the potential and shape of the well change and, in particular, the height of the barrier corresponding to the uppermost level of charges in the well changes. The depth of the barrier of the upper levels of charges filling the potential well can be varied by changing the effective voltage drop on the capacitor, the thickness of the oxide dielectric layer, and also the concentration of doping in the semiconductor. The thickness of the silicon oxide layer is usually 10 nm, the electrical voltage pulse about 10 V, and the limiting surface density of charges accumulated in a dynamic mode is about 10^{12} electrons/cm^2.

If two miniature capacitors are placed next to each other in such a way that their depletion regions overlap, the potential wells of the two capacitors will become connected and the accumulated charge will flow into the deeper potential well. This transfer of charge provides the basis of the operation of a charge-transfer device.

In a three-phase system[1] the transfer of charge from one miniature capacitor to another occurs as follows (Fig. 2). During the first phase let the signal charge be under electrode 1, which has a higher potential than electrodes 2 and 3. If the same potential is applied to electrode 2, the signal charge will flow along the well under electrodes 1 and 2. If in the second phase the voltage is removed from electrode 1, then the charge completely flows into the potential well under electrode 2. After a corresponding change of the potentials on electrodes 2 and 3, during the third phase the signal charge will flow into the potential well under electrode 3. Then the sequence of phases is repeated periodically in time. The set of electrodes of the linear matrix of miniature capacitors is broken up into three groups. To each group trapezoidal voltage pulses are fed from one of three generators, the clock pulses from which are shifted in phase by 120° relative to each other. Unidirectional transfer of charge in a two-phase system is achieved by the fact that the potential under the gate has an asymmetric distribution. Therefore the charge carriers accumulate in the deeper part of the potential well, and transfer of charge occurs only under the closest gate. The nonuniform distribution of potential in the well is produced by means of variations in the thickness of the dielectric layer or local increase of the concentration of doping near one edge of the gate. The most widely used arrangement utilizes a different thickness of the dielectric layer under the gate, and in particular, CTDs with two levels of metallization.[1-3] Ion-implantation methods or structures with undercut isolation[6] are also used. All two-phase systems can be converted to one-phase if a dc bias is applied to one of the pulse buses.[7] The frequency of the clock generators is 10^7–10^8 Hz.

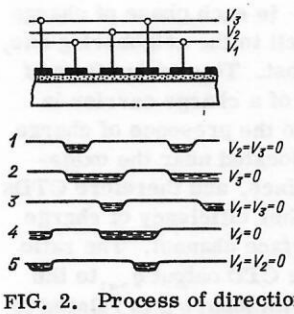

FIG. 2. Process of directional transfer of charge along a chain of MOS capacitors by means of a three-phase system: the voltage V_1 is supplied to electrode 1, V_2 to electrode 2, and V_3 to electrode 3.

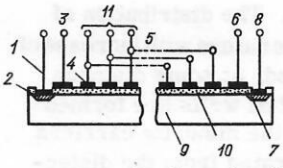

FIG. 3. Basic elements of a charge-transfer device: 1—input electrode, 2—source in the form of a diffusion region, 3—input controlling gate, 4—gates of CTD chain, 5—three-phase voltage-input system, 6—output gate, 7—output semiconductor junction, 8—output electrode, 9—semiconductor, 10—dielectric layer, 11—electrodes connected with three clock-pulse generators.

A charge-transfer device consists of three main elements (Fig. 3): 1) an input section which contains a source of minority carriers of the semiconductor and a gate which transports the charge from the source to the first miniature capacitor; 2) a charge-transfer register with miniature capacitor control electrodes; and 3) an output section which contains a gate and an output semiconductor junction in which is generated a voltage pulse with an amplitude proportional to the number of transferred minority charge carriers of the semiconductor.[3]

Both transmission and storage of information in a CTD are carried out by means of minority carriers. In contrast to CTDs, storage of information in traditional semiconductor devices is carried out by means of minority carriers, but the transfer of charge is by means of majority carriers. Therefore it is always necessary to transform the information from one form to the other. This conversion occurs in the diffusion region of the semiconductor.

In addition to CTDs with a surface channel, described above, there are CTDs with a bulk (buried) channel[1,8,9] (Fig. 4). Under the dielectric layer there is placed a layer of semiconductor with a conductivity type opposite to that of the substrate. A *pn* junction arises which is located at a small depth and which is con-

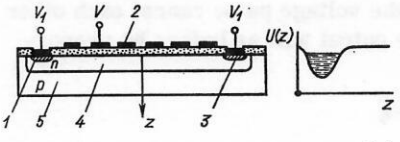

FIG. 4. Charge-transfer device with bulk channel: 1—input diode, 2—electrodes, 3—output n^+ diode, 4—bulk (buried) charge-transfer channel in semiconductor with n conductivity, 5—substrate in the form of semiconductor with p conductivity; the shape of the potential along the z coordinate is shown at the right.

nected in the reverse direction. The distribution of the potential has a nonmonotonic nature with increase of distance from the dielectric, and, at some distance from the dielectric, deep potential wells are formed under the gates. In this design the minority carriers move along a bulk channel separated from the dielectric-semiconductor boundary surface. The voltage applied to the n layer is chosen so that the region of space charge of the reverse-biased pn junction encompasses the entire n layer and the n layer is depleted. The inefficiency of charge transfer in the bulk channel is $\varepsilon = 10^{-5}$, but the limiting value of charge accumulated in a CTD with a bulk channel is significantly smaller than in a CTD with surface charge. CTDs with a bulk channel can operate efficiently at a clock-pulse repetition frequency up to 10^8 Hz.

In 1946 Schlesinger[10] pointed out for the first time that analog signals can be stored in the form of charges of various magnitudes in a chain of miniature capacitors and that the chain as a whole can be shifted along the line of capacitors from one to another by means of electrical switches controlled by clock pulses. This idea has now been realized at the technical level in the form of charge-transfer devices.

Semiconductor devices form an independent group of CTDs. Each element of these devices consists of an MOS transistor, the operation of which is controlled by a two-phase circuit (Fig. 5). These are called bucket brigades.[1,2] The islands of diffusion region located under each gate serve as a drain for one gate and as a source for the neighboring one. Charges are stored in the back-biased p regions. Under the influence of a pulse of electric field applied to the gate, one of the potential barriers of the well, for example the left one, is lowered, and charge flows from one potential well to the other. The direction of flow of charge arises as the result of a definite location of the gates with respect to the diffusion islands.

Charge-injection devices, which are also a variety of CTD, contain islands of p-conductivity between the electrodes, but the substrate has n conductivity (Fig. 6). In the scanning process the voltage is removed from the gate and the charge stored under this gate is injected into the substrate in the form of minority carriers, creating a pulse of current in the external circuit. As a result of the large coupling capacitance, the change in voltage in the clock pulse produces parasitic pulses of current in the external circuit. However, if the current as a function of time is integrated over a time somewhat exceeding the duration T of the controlling pulse, then the current pulses from the rise and fall of the voltage pulse cancel each other and the signal at the output will as before be proportional to the charge. An important deficiency of a charge-injection device is its high output capacitance. We recall that in an ordinary CTD the charge follows into a single output diode of very small size for the entire chain of the register; the harmful influence of clock-voltage pulses on the output signal is very small and can be further decreased.

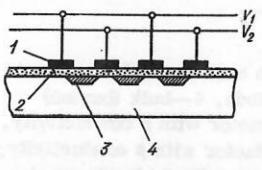

FIG. 5. Bucket brigade: 1—electrode, 2—dielectric layer, 3—diffusion regions, 4—semiconductor.

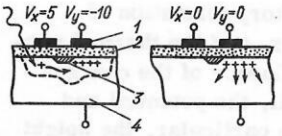

FIG. 6. Principle of action of charge-injection device: 1—gates, 2—dielectric layer, 3—islands of p conductivity, 4—semiconductor with n conductivity.

2. PHYSICAL PROPERTIES OF CHARGE-TRANSFER DEVICES

Limiting charge density.[1] The requirements of obtaining high signal amplitude at the output of a CTD and preserving the small size of each cell are mutually exclusive. The smaller the size of the MOS miniature capacitor, the smaller is the height of the signal and the poorer the signal-to-noise ratio. The universal parameter which limits the choice of a compromise solution is equal to the limiting surface density of signal charges of the CTD.

The charge q which can be stored in a potential well is simply related to the electrical capacitance of a unit area of the dielectric layer C and the height of the electric voltage pulse U:

$$q/\sigma = UC; \quad C = \varepsilon_0 e/d, \tag{1}$$

where σ is the area of the active part of the electrode, e is the dielectric constant of the dielectric layer, and d is its thickness. For voltages close to breakdown we have

$$U^{\max}/d \approx 10^6 \text{ V/cm} \; ; \quad q_{\max}/\sigma \approx 10^{13} \text{ el/cm}^2. \tag{2}$$

Usually no more than 3×10^6 electrons are stored in each potential well; for a clock frequency $f_c = 1$ MHz this corresponds to an electric current of about 1 μA. The charge which can be stored in each potential well is somewhat less than the limiting value given above. In CTDs with a bulk channel located at a depth of about 5 μm, the effective electrical capacitance of the dielectric layer is less than in CTDs with a surface channel.

Charge transfer efficiency.[1] In each phase of charge transfer from one potential well to the neighboring one, a fraction of the charge ε is lost. This is due first of all to the limited rate of drift of a charge carrier in the semiconductor layer and to the presence of charge traps. Most of the traps are located near the oxide-semiconductor separation surface, and therefore CTDs with a bulk channel have a higher efficiency of charge transfer than CTDs with a surface channel. The ratio of the quantity of charge at the CTD output q_{out} to the quantity of charge arriving at its input q_{in} is related to the transfer inefficiency ε as follows:

$$q_{out}/q_{in} = (1-\varepsilon)^N \approx 1 - N\varepsilon, \tag{3}$$

where N is the number of steps of the CTD. Usually $\varepsilon = 10^{-4}$.

If the zero signal corresponds to an empty potential well, then the initial signal-train pulses fed to the CTD undergo additional distortions which are equivalent to inefficient charge transfer. The charge of the first packet goes partly into filling the traps which exist in the channel and which are unfilled before arrival of the signal. This loss of charge is higher, the greater is the time interval between two signal trains. In order to reduce this loss, the zero value of the signal is shifted and the intervals between two signal trains are filled with charge packets of constant magnitude. This method is called the "nonempty zero" (bias-charge) method.

Transfer of charge along the chain of miniature capacitors of a CTD occurs under the influence of thermal diffusion, self-induced drift of charges, and the longitudinal components of the fringing electric field. In thermal diffusion the distribution of charge density in space along the CTD matrix is described by a cosine wave with a zero at the edge of the potential jump and an amplitude decaying exponentially with time with a time constant

$$\tau_{\text{therm}} = 4L^2/\pi^2 D, \qquad (4)$$

where D is the coefficient of diffusion of charge carriers in the semiconductor layer; L is the width of the electrode from under which charge flows into the potential well located under a neighboring electrode.

If the quantity of charge in a packet is sufficiently large, the carriers experience electrostatic repulsion which is weakened with decrease of the volume density of the charges. The effective time of self-diffusion of the carriers is

$$t_0 = (\pi/2)\, L^2/\mu\, (V_1 - V_0). \qquad (5)$$

where μ is the mobility of the charge carriers; $(V_1 - V_0)$ is the initial signal voltage. The mobility of electrons in a semiconductor for an impurity density 5×10^{14} cm^{-3} is $\mu = 1.2 \times 10^3$ cm^2/volt-sec. The rate of transfer of charge under the influence of thermal diffusion for $d = 100$ nm is comparable with the rate of self-induced drift at a charge density of about 10^{10} cm^{-2}.

The principal advantage of bulk-channel CTDs is that the electric fringing fields are significantly greater here than in CTDs with a surface channel. This permits a high efficiency of charge transfer to be obtained even for very low clock frequencies. The acceleration of the charge-transfer process in CTDs with a bulk channel occurs because between the region where the signal charges are propagated and the surface separating the semiconductor and the dielectric there is a layer of depleted silicon. The transfer inefficiency for CTDs with a bulk channel is usually $\varepsilon = 5 \times 10^{-5}$ for a clock frequency 10 MHz. It is expected that CTDs with a bulk channel will be able to operate at clock frequencies of about 10^9 Hz. At low clock frequencies dynamic outflow of charge sets in. In order to reduce this effect a tetrode electrical system of charge transfer in a bulk channel with decoupling of the voltage source is used. The same result is obtained if instead of ordinary transistors one uses injection field-effect transistors. Systems of this type have fast action, are stable with time, have a stable threshold, and also can work at controlling voltages of 2 volts.

At very low clock frequencies the decrease in the efficiency of the charge-transfer process is due to thermal diffusion of charge carriers into the channel or through the potential barrier. The potential of the source becomes lower than that of the charge-transfer channel, and charge drain occurs at a rate which decreases logarithmically with time. CTDs with a bulk channel are subject to the action of traps to a smaller degree than those with a surface channel. The inefficiency of charge transfer along a chain of CTDs leads to the result that the signal bandwidth B which can be transmitted without distortion is

$$B = (f_c/2)\, I_0(2N\varepsilon) \exp(-2N\varepsilon), \qquad (6)$$

where $I_0(x)$ is a modified Bessel function:

$$I_0(x) = \sum_{k=0}^{\infty} \left(\frac{x^k}{2^k k!}\right)^2 .$$

Dark current and noise. CTDs have low noise, and this is one of the reasons for the great interest in these devices on the part of workers in many fields of science and technology.[1,2,11] It is because of this physical characteristic that CTDs are successfully used as photodetectors in streamer chambers[12] and in television systems under conditions of low illumination.[3,13,14,68]

Noise in CTDs arises as the result of random fluctuations of the number of charge carriers in the process of flow along the chain of miniature MOS capacitors, and also in the stages of injection and readout of signals. CTDs used as image detectors also have photon noise which accompanies the process of photoelectron production. The least fluctuation noise is provided by CTDs with a bulk channel. At a temperature of −50°C this noise is equivalent to ten electrons.

The noise in the injection stage depends on the electrical arrangement for introducing charge and on the shape of the controlling pulses fed to the input diode. Noise arising in the signal-readout systems is similar to the noise arising in semiconductor particle detectors. Reset noise in an amplifier has a mutual correlation and can be reduced by using correlated double-sampling logic. The lowest noise is provided by distributed amplifiers with a floating gate.[15,16] Finally, CTDs have geometric noise which arises as the result of spread in the capacitance values of the sources providing the bias charge in each column of the CTD matrix. The total spread due to noise in the input and output circuits and also in the process of charge flow in the CTD is about 500 electrons at room temperature.[17]

Electron-hole pairs are continually produced under the action of thermal vibrations of the lattice in the volume of the semiconductor. Noise charges arising at the semiconductor-dielectric boundary, and also in the depletion region and in the semiconductor layer

extending from the boundary to a depth equal in order of magnitude to the minority-carrier diffusion length, gradually fill the potential wells of CTDs. The effective filling time of a well is

$$t_{\text{fill}} = C_{\text{ef}} \Delta V / i_d, \quad (7)$$

where C_{ef} is the effective storage capacitance of a unit area occupied by the potential well, i_d is the dark-current density, and ΔV is the height of the barrier between the potential wells. Usually $t_{\text{fill}} \approx 1$ sec. The nonuniformity of the dark current determines the observation threshold. At room temperature this threshold is about 1000 electrons.

The lattice levels responsible for thermal production of electron-hole pairs are concentrated near the central part of the forbidden band of the semiconductor. Therefore the temperature dependence of the dark current has the form

$$i_d = i_{d_0} \exp(-E_f/2kT), \quad (8)$$

where E_f is the width of the forbidden band of the semiconductor. The dark current decreases roughly by a factor of two on reduction of the temperature every 10°C. At $t = -50$°C and with a 10% nonuniformity of the cells of the CTD, the observation threshold is eight electrons. Fluctuations in the thermal generation process produce transient noise whose dispersion is equal to the rms value of the dark current.

The spectral density of noise signals[18] arising in a resistance under the influence of the thermal motion of the charge carriers has a constant value up to frequencies $f_{\max} = kT/\hbar$, where $\hbar$ is Planck's constant. At room temperature $f_{\max} = 10^{13}$ Hz. The spectral density of thermal noise does not depend on the value of the current flowing through the resistance if the value of the latter and the temperature do not depend on the current value. This condition is satisfied if the average drift velocity of the charge carriers is small in comparison with the velocity of their thermal motion. The spectral density of fluctuation noise has a constant value up to frequencies near 10^{10} Hz for a semiconductor junction width of 1 μm and a carrier velocity of 10^7 cm/sec.

In active semiconductor elements at low frequencies, noise is observed the spectral density of which varies inversely in proportion to the frequency ($1/f$). One of the causes of this noise is the process of capture of charge carriers by deep-lying traps.[1]

Interference from clock pulses. The clock pulses which control the shift of charges in a CTD produce interference in the output circuits. There are several methods for reducing this interference, based on use of differential switching. For example, in bucket-brigade CTDs the amplifier gates are connected to opposite phases of the clock-pulse generator, alternating with every gate of the chain.[19] The clock pulses cancel each other, and a signal proportional to the stored charge is formed at the amplifier output. The spikes from the rise of the clock pulses are taken out in a high-frequency filter.

Radiation. CTDs are subject to the action of intense radiation. It has been established[3] that a CTD with a surface channel will withstand irradiation of no more than 10^3 rads, while a CTD with a bulk channel will stand no more than 10^4 rads of γ rays from cobalt 60.

3. TECHNICAL CHARACTERISTICS OF CTDs[1,2,20-25]

The height of the controlling clock pulses of voltage in CTD systems is 10–20 V and places an upper limit on the signal height in CTDs. For a linearity of 1% the maximum signal height is 1–5 V.

The maximum bandwidth of the input signal is equal to half of the clock-pulse repetition frequency and is about 20 MHz. The minimum clock-pulse repetition frequency is 100 Hz.

The power required is at least 4 μW/bit.

The maximum delay time of the signal is 1–10 sec.

The maximum number of elements in a CTD chain is about 2000.

The photosensitivity of CTDs is about 500 $\mu A/lm$ and is close to the characteristics of other types of silicon photodetectors.

The minimum dispersion of the noise is ten electrons per packet.

The minimum charge-transfer inefficiency is 5×10^{-5}.

The sensitivity of an amplifier with a floating gate is 20–100 μV for one electron of charge.

4. USE OF CTDs FOR SIGNAL PROCESSING

A chain of CTDs is a discrete analog shift register which has broad ragions of application. Electrical pulse delay lines constructed of CTDs have a number of interesting properties.[1,2,21,26,27] For example, the delay time in a CTD changes with change of the clock-pulse repetition frequency. The product of the bandwidth B and the delay time T_0 is related to the number of elements N in the delay line as follows:

$$BT_0 = N/2. \quad (9)$$

In turn N is limited in the upper direction by the transfer inefficiency ε. For $\varepsilon = 2 \times 10^{-4}$, $N \leqslant 500$.

In order to increase the BT_0 of a signal transmitted along a delay line of CTDs, use is made of several parallel chains. In Fig. 7 we have shown a schematic representation of such a system with a series-parallel-series arrangement of M chains, each of which contains N cells. The number of transfer phases for each charge packet is $M+N$, and the total number of elements is MN. Usually $MN \geqslant 10^3$. Delay of a video signal by 16 μsec is accomplished by a system with $M = 106$ and $N = 128$.

A vertical analog delay can be used as an indicator of moving objects observed by means of a radar system.[31] For this purpose the signal reflected from the first pulse is subtracted from the signal reflected from the next pulse. The signals from fixed objects are suppressed and only moving objects are imaged.

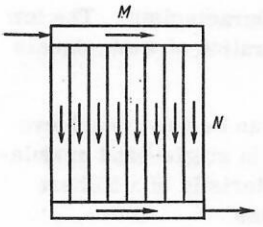

FIG. 7. Schematic arrangement of CTD registers with series-parallel-series arrangement of M chains of N cells.

Delay lines employing CTDs are utilized in an ultrasonic acoustic imaging system[28] operating on the principle of electronic focusing. A set of delay lines with a delay time varying quadratically from channel to channel corresponds to a definite curvature of a spherical acoustic wavefront. It the clock frequency in all the delay lines is changed, the point of focus in space shifts. If the acoustic wave is traveling at an angle to the line of acoustic field detectors, then a change of the clock frequency in a system with linear variation of the delay time will lead to scanning over an angle θ to the z axis. If two systems with different clock frequencies are used, then scanning in angle will be carried out both to the left ($f_1<f_2$) and to the right ($f_1>f_2$) of the z axis. A set of three delay lines employing CTDs can be arranged on a single silicon cyrstal which performs the function of an electronic focusing lens for the acoustic field (Fig. 8).

Multiplexing systems with separation of the channels in time are conveniently realized by means of CTDs. Information is read into the CTDs in parallel and read out in series. The intensity of cross interference between different channels is determined by the transfer inefficiency ε. The main advantage of such a system is its economy.

An important characteristic of CTD delay lines is the fact that the delay efficiency does not depend on the spectrum of the signal, and such lines can be used in analog recursive filters and transversal filters. A diagram of a recursive filter[1] in which the signal is

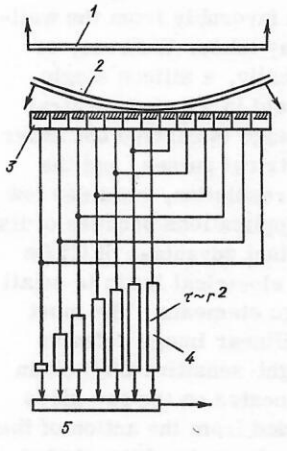

FIG. 8. Electronic focusing lens for an acoustic field: 1—sound wavefront, 2—scattered wavefront from point object, 3—set of transmitter-receivers of the acoustic field, 4—delay lines employing CTD registers, 5—scanning register.

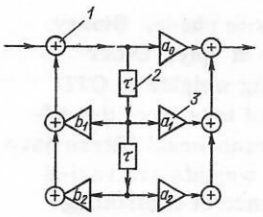

FIG. 9. Diagram of simplest recursive digital filter: 1—adding elements, 2—elements of delay line, 3—multiplication elements.

shifted both forward and backward in time is shown in Fig. 9. The transfer characteristic of such a filter is given by the z-transform:

$$H(z^{-1})=\sum_{k=0}^{N} a_k z^{-k}/(1-\sum_{k=1}^{N} b_k z^{-k}). \qquad (10)$$

Here the roots of the polynomial in the numerator provide the zeros of the transfer function, and the roots of the polynomial in the denominator provide its poles.

In a transversal filter $b_k=0$ for all k. In Fig. 10 we have shown the simplest examples of recursive and transversal filters of first order. The duration of the pulse response of transversal filters employing CTDs amounts to a fraction of a second, and the transmission bandwidth is 10 MHz or more. The frequency characteristics of a filter can be varied over wide ranges.

CTD filters have a number of important advantages over digital filtering systems employing computers. These are: low relative cost (≈1 : 100), the possibility of preparation of compact matched filters and band filters, and simplicity of planning any forms of CTD filters.

Transversal filters[29,30] employing CTDs are used successfully to achieve a discrete Fourier transform, a Hilbert transform with single-band modulation, etc.

A transversal filter with programmed weights can be combined with a microprocessor. The pulse response of a transversal filter determined by a set of weights a_k, where $1\leq k\leq N$, is

$$g(t)=\sum_{m=1}^{N} a_m \delta(t-m\tau). \qquad (11)$$

where τ is the delay time per phase.

In order to achieve the required values of weights in CTD filters, the electrodes of the storage capacitance are cut into two parts so that the lengths of the parts are in the ratio $(1+a_m)/(1-a_m)$. The signals from

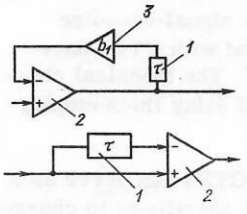

FIG. 10. Diagram of simplest recursive and transversal digital filters: 1—delay-line element, 2—adding element, 3—multiplication element.

each part are connected in opposite phase. Binary codes[1] are achieved particularly simply. Other methods also exist for introducing weights in CTD filters, for example, by means of taps from the diffusion regions. In particular, transversal filters have been built in such a way that the weights are varied programatically under the influence of controlling voltages. It is remarkable that the pattern of location of the electrode cuts of a transversal filter employing CTDs coincides completely with the form of the discrete function $g(t)$ of the pulse response of the transversal filter. If a discrete sequence $f(t)$ is fed to the input of a transversal filter, then at its output there appears a signal

$$s(t)=\sum_{t'=1}^{N} f(t')\,g(t+t')=f(t)*g(t), \qquad (12)$$

which is equal to the discrete correlation function of the signal $f(t)$ and the transversal filter pulse response $g(t)$. Correlators employing CTDs are characterized by the following parameters: weighting accuracy 1:200, storage time at room temperature 1 sec, and clock frequency 3 MHz. Up to 4×10^4 discrete signal readings are processed simultaneously with an accuracy of 1%. It has been shown that CTD correlators can operate at the bit level.[21] For this purpose several double correlators are used, each of which carries out transformations in the corresponding digit with weights ±1. Extraction of results from the various digits is scaled by means of different load resistors or by combination of CTDs having different physical areas. The required accuracy in calculation of the correlation is provided by a system consisting of four double correlators.

Such a system of double correlators is equivalent to a high-speed peripheral computer device with operations of multiplication and addition. In combination with a microprocessor, such a system can compete successfully with a universal computer. A system of 128 double correlators is capable of carrying out more than a thousand eight-digit multiplication and addition operations in a time of 1 μsec. It has been noted that such a system supplied with program control can carry out matrix inversion and solution of other similar problems.

Matched filters intended for separation of a signal of known shape in a background of noise are extensively used in communications technology. The pulse characteristic of a matched filter is equal to the received signal whose discrete components are arranged in inverse sequence. Transmission of signals of great duration and reception of them by matched filters permits a substantial increase in signal-to-noise ratio. Matched filters constructed with CTDs have characteristics close to ideal.[1,17] The technical characteristics of matched filters and delay lines employing CTDs coincide.

Transversal filters employing CTDs can serve as a band-pass filter having minimum sensitivity to charge-transfer inefficiency in the CTD. The frequency of the pass band of a CTD filter changes with the clock-pulse frequency. The possibility exists of obtaining a filter with a linear phase-frequency characteristic. The low noise level of CTDs permits filtration of weak signals to be performed.

A transversal filter of CTDs can be used to achieve the Hilbert transformation used in single-band modulation systems. The pulse characteristic of a Hilbert filter is determined by the weights

$$a_m=[m-(N+1)/2]^{-1}, \quad 1\leqslant m\leqslant N, \qquad (13)$$

where N is odd, and the signal at the filter output, which is equal to

$$s(t)=\sum_{k=1}^{N}\frac{f(t-k+1)}{(k-(N+1)/2)}, \qquad (14)$$

undergoes a delay $N\tau/2$. As a consequence of the discrete nature of the transformations carried out by means of CTDs, the imaginary part of the spectral characteristic of a Hilbert filter has a discrepancy from the ideal characteristic in the low-frequency region.[1]

With the appearance of CTDs it has become possible for the first time to prepare the entire equipment for processing of analog signals by means of integrated semiconductor technology.

5. CTDs AS IMAGE PHOTODETECTORS

CTDs have a high quantum efficiency and self-scanning properties in readout of discrete analog information. Therefore they are used as efficient and fast converters of images into a discrete video signal. The process occurs through two phases: storage and readout. During the storage phase no clock pulses are fed to the CTDs. Electron-hole pairs are produced in the CTDs under the action of photons. Into each potential well there flow minority charge carriers arising in the vicinity. During the readout phase the light flux onto the CTD is cut off, clock pulses are fed in, and consequently the packets of photocharge shift along the CTD chain.[1,2,20] A set of charge pulses quantized in amplitude represents a video signal in a given line of an image.

The conversion of an image into a video signal by means of a CTD chain differs favorably from the well-known prototypes: cathode-ray tubes, Vidicons, or photodiode matrices. Specifically, a silicon single crystal has a high quantum yield in a broad spectral region, the scanning of the image is carried out under the action of low-voltage electrical pulses, and the CTD matrix has high special resolution, requires low power, and is convenient in applications because of its compactness. Another important advantage of CTDs is the fact that the number of electrical leads is small ($\lesssim50$) for any number of image elements. The most efficient linear system is a bilinear image detector which consists of a central light-sensitive CTD chain and two CTD shift registers located on the two sides of the central chain and shielded from the action of the light flux (Fig. 11). The even elements of the chain are connected to the left register, and the odd elements to the right register.[1] In transmission of the photocharges from the central chain to the shift registers

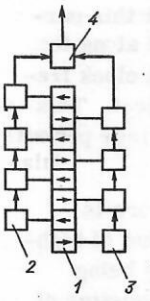

FIG. 11. Bilinear line image sensor based on CTDs: 1—light-sensitive chain, 2—left register, 3—right register, 4—output element.

a time equal to the total clock period is expended. Then the central chain goes over again to the mode of storing photocharges produced by the light of the next line of the image. In the bilinear system a two-phase readout logic is usually used. Bilinear systems with a number of elements in the chain equal to 500, a spatial resolution of 30 μm, and a dynamic range of $3 \times 10^3 : 1$ have been built.

The analog structure of the signals of a CTD photodetector permits the most typical forms of processing of video signals to be carried out by means of CTDs: discrete Fourier transform, multiplex readout, moving-target indication, and subtraction of a constant dark-current pattern.[21,31,37]

The matrix system for conversion of an image into a discrete video signal can be constructed by various methods. The simplest CTD matrix consists of a set of CTD lines (Fig. 12). The video signals from each horizontal line are read consecutively into a vertical register, and from it into an output diode. A CTD matrix of dimensions 32×44 has been constructed in this arrangement. In a double CTD matrix the storage of photocharges is carried out in the upper matrix, which is assembled from vertically arranged registers. The lower matrix, which has a common horizontal register, is intended for storage and readout of the photocharges (Fig. 13). First the photocharges move rapidly from the frame matrix to the lower matrix, and then they are read out consecutively line by line in the horizontal direction.[20]

Interlaced scanning is also possible, corresponding to standard contemporary television. For this purpose the number of charge packets in successive half-frames is doubled in a vertical direction without changing the total number of elements in the CTD matrix. Thus,

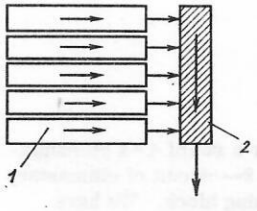

FIG. 12. Simplest matrix of image photodetectors employing CTDs: 1—line image sensor, 2—vertical register shielded from light.

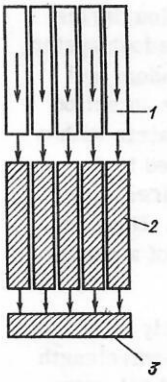

FIG. 13. Double matrix of image sensors employing CTDs: 1—upper matrix, in which storage of photocharges is carried out; 2—lower matrix, intended for storage and readout of photocharges; 3—scanning register.

each vertical cell is used to obtain video signals of two lines on the screen, in contrast to the traditional system where for each line there is an individual channel. Systems have been constructed with 220×256 elements of an interlaced image with an image-element size 30×30 μm^2. The required power is 1.5 watts. Pocket television cameras with a number of elements 100×100 and a resistivity 1 *lm* went on sale in 1973.

The desirability of use of CTD matrices in television is due to the fact that in CTDs there is no problem of accurate coincidence of the sweeps in color television cameras in three tubes.

In a three-phase readout system it is possible to form six separated images imbedded in each other. However, in images obtained by this method a phenomenon equivalent to the stroboscopic effect is observed.

Devices with charge injection possess a fundamentally different readout logic. Here two-coordinate addressing is used (Fig. 14). Charge injection occurs in those cells in which the voltages on the horizontal and vertical bus bars coincide and are equal to zero. The output capacitance of a device with charge injection is equal to the capacitance of a single row and a single column if during the readout all remaining bus bars are at a floating potential. The readout noise in a charge-injection device is high, and therefore this type of device can be used only at high levels of illumination.[1,13,20,32]

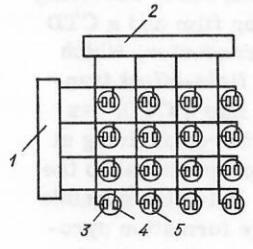

FIG. 14. Diagram of image-scanning system in a charge-injection device: 1—generator of scanning voltage pulses in the right electrodes of the cells, 2—generator of scanning voltage pulses in the left electrodes of the cells, 3—left electrode of the cell, 4—right electrode of the cell, 5—circuit of an elementary cell.

An important advantage of a charge-injection device with two-dimensional addressing of the readout system is that here it is possible to use pseudorandom and also multiplexed readout systems. Charge-injection devices have been built in the form of a matrix with a number of image elements 248×244, cooled to a temperature $-70°C$. Charge-injection devices have high reliability and are simple to prepare. However, the dynamic range is 500:1, and the size of a charge-injection device is relatively large.

The effective region of spectral sensitivity of silicon CTD photodetectors is limited on the long-wavelength side to a wavelength of 1 μm, and on the short wavelength side to about 0.4 μm. The quantum yield of a silicon single crystal is close to unity, and the sensitivity to illumination is about 500 $\mu A/lm$. However, the real quantum yield turns out to be lower than this if special measures are not taken to increase it. One of these special measures consists of directing the light flux to the back side of the CTD matrix in order to avoid absorption and reflection of light from the front face of the matrix. In backside illumination the quantum yield is 0.5 for wavelengths 0.5–0.9 μm and 0.9 at a wavelength 0.7 μm. The falloff on the short-wave side is due to recombination occurring both in the semiconductor layer and at the rear boundary surface, and the falloff on the long-wavelength side is due to incomplete absorption of infrared radiation in the thin semiconductor layer. CTD systems of dimensions 160×100 image elements have been built with backside illumination.

However, an interlaced scanning system cannot be combined with backside illumination of the semiconductor layer, since here special shields are necessary to prevent diffusion of carriers directly to the storage register.

Thin-layer CTD detectors have been used in electron beams, where detection occurs with a gain up to several hundred at sufficient electron energies. The same device can be used for detection of protons or neutrons. However, the characteristics of such a device deteriorate with time as the result of destruction of the silicon lattice and decrease of the minority carrier lifetime.

CTD photodetectors can be used as systems for formation of thermal images.[3] However, the most promising system is a hybrid system whose receiving portion consists of a photoconducting film and a CTD matrix. Each element of the photoconductor, which serves the function of the gate of a field-effect transistor, controls the flow of charge into a CTD. Its potential, and also the quantity of charge arriving at the potential well of the CTD, are proportional to the intensity of the infrared radiation. It is also possible to use as targets for thermal-image formation pyroelectric crystals whose spontaneous electrical polarization along one of the crystalline axes changes with temperature. The CTD matrix is cooled to a temperature 77 K.

A matrix of CTD photodetectors can be used to photograph uniformly moving objects.[31] For this purpose the columns of the matrix are oriented along the velocity vector of the object and the readout clock frequency coincides with the velocity of the object. This combined mode of time delay and signal storage permits increase of the signal-to-noise ratio.

The resolution of matrix CTD photodetectors is approximately a factor of two poorer than that of high-quality television systems, but is constantly being improved. The frequency-contrast characteristics of a CTD photodetector depend on the architecture of the readout. In systems with frame transfer the frequency-contrast characteristic varies with a spatial frequency substantially steeper than in a system with line transfer. Usually frame transfer occurs with a rate 30 frames per second with a photoelectron storage time equal to 1/60 sec. The time for shift of the charges into the readout matrix is 1/600 sec.

At low levels of illumination the signal-to-noise ratio in CTD photodetectors is poorer than in cathode-ray tubes. The resolution and the signal-to-noise ratio are interrelated at low illumination levels.

An important deficiency of CTD photodetectors is the fact that at high light-intensity levels, overfilling of the potential well occurs and the excess charge goes into the neighboring potential wells. This leads to a smearing of the image and to appearance of bright bands along the CTD registers. In order to suppress the outflow of excess charge and to reduce the smearing of the image, drains are introduced in the form of reverse-biased diodes with a definite bias voltage and a low-impedence circuit. These drains are placed between neighboring transfer channels.

The technology or preparation of CTD photodetectors and the results of experimental tests are given in Refs. 23 and 33.

In Fig. 15 we have shown a parallel-injection circuit for a 4×4 array. The voltages applied to the electrodes of a row exceed the voltages on the electrodes of a column, and therefore the signal charge accumulated in the uninterrogated cells does not affect the

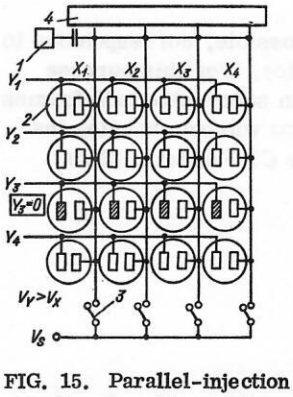

FIG. 15. Parallel-injection circuit for a set of 4×4 elementary cells: 1—voltage-pulse generator, 2—circuit of elementary cell, 3—electronic switches, 4—scanning block. We have shown the moment at which in the third row all the left electrodes are at zero potential and all the vertical lines are at a floating potential.

column cells. Before beginning the process of interrogation of a row, voltage is applied to all rows, and the voltages on the columns are discharged to a reference voltage V_S by means of four switches and subsequently remain floating. In the row undergoing interrogation, the voltage is removed, as a result of which the signal charges in all cells of the row transfer to the column electrodes. Here the voltage in each floating line changes by an amount equal to the ratio of the signal charge to the capacitance of the column. After this the horizontally scanning register reads the voltage in all cells of the column, and the video signal obtained is sent to a preamplifier. Here the input voltage to the preamplifier is discharged to a reference level before interrogation of the horizontal register is begun.

At the end of each interrogation of a line, the entire charge of this row is injected into the substrate by application of zero potential to the entire column through two switches. Another very interesting possibility also exists. The injection operation is not carried out completely, but the signal charge is transferred back under the row electrodes. This readout scheme is called nondestructive.[13]

The parallel injection scheme permits a high readout rate. Injection photodetectors of size 244×248 have been prepared on a crystal, together with a preamplifier, and both the injection and nondestructive readout modes have been tested in association with a television system at a frequency 5 MHz and a frame speed 60 fields per second.[13]

In order to provide buried collection of the injected charges, charge-injection devices used as a photodetector matrix are prepared in epitaxial layers. If the thickness is comparable to the matrix step, then the main portion of the injected charge is collected by the reverse-biased epitaxial junction. In this case the effect of cross modulation of the injection process turns out to be minimal, the signal-charge collection time decreases to 10^{-8} sec, and as a result of electrical insulation of the cells from each other the image-smearing effect is substantially reduced.

In the nondestructive readout mode the charge-injection process does not occur in general, and image smearing does not arise. Tests of the nondestructive readout mode have shown that at a temperature −73°C the buried image was preserved for three hours after 3×10^5 repeated readout operations. This is equivalent to loss of only one elementary carrier per cycle in each cell of the matrix. Finally, in a charge-injection device the linear noninterchangeability effect typical of photographic and other materials is absent. It has been shown that the storage of a large number of small packets of photocharge is characterized by a strict linear dependence from 1/30 sec to three hours.[13]

Use of transparent electrodes of metallic oxide for charge-injection devices with front illumination permits a uniform (±10%) spectral characteristic to be obtained for these devices in visible light.

The advantage of transparent electrodes of metal oxide (indium oxide or tin oxide) is that it is possible to produce by means of planar technology a cell of a charge-injection device in which systems of horizontal and vertical electrodes cross and in which the light is incident from the front. A compact charge-transfer device in the form of a 32×32 matrix has been prepared from cells of size 30×40 μm^2.[34]

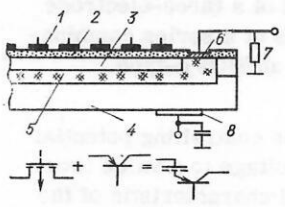

FIG. 16. A charge-transfer device with three electrodes: 1—controlling gate, 2—dielectric layer, 3—epitaxial n^- layer, 4—n^+ substrate, 5—bulk collector channel with p conductivity, 6—output electrode of bulk channel, 7—resistor, 8—collector.

A new variety of charge-injection device contains three leads.[35] In this device the scanning element is a bulk channel in the form of a p-type band on an n-type substrate. The band has a lead to the surface at one end. The channel is a collector of injected minority carriers stored under the gate. In such a system the useful signal and the noise signal proceed by different paths with fixed spatial distribution. Readout in a system with three leads is accomplished in such a way that no switching transients arise. This leads to a decrease of the signal-to-noise ratio in comparison with the traditional design of a charge-injection device. Two-dimensional addressing is greatly simplified in a three-terminal system. A diagram of the design with three electrodes is given in Fig. 16. Each cell consists of a gate of polycrystalline silicon on an oxide-dielectric layer, under which lies an epitaxial n^- layer and then a bulk collector channel with an output electrode on the surface at one end.

Still further below is located the n^+ substrate. The purpose of the bulk p-type collector band is to collect injected minority charge carriers which diffuse through the epitaxial layer. The third electrode is the substrate, which achieves access to the epitaxial n^- layer by means of a volume n^+ semiconductor which encompasses the bulk p-type band on all sides.

The collecting electrode is grounded through an output resistor R_L. A positive bias voltage V_{SS} is applied to the substrate. A negative voltage V_G which is periodically reduced to zero for a short time is applied to the gates. During this time charge from the capacitance flows through the gate capacitance of the silicon, except for the p-type band, to the grounded n^+ substrate. At the same time the injected minority carriers diffuse from the plane separating the silicon and the oxide through the epitaxial n^- layer, where part of them recombine with majority carriers and part are collected in the p-type band. Similar processes occur in a bipolar pnp transistor in which the base function is filled by the epitaxial n^- layer and the collector function by the buried substrate. Instead of a diffusion emitter there is a time-dependent field-effect injection

junction. The electrical circuit of a three-electrode charge-injection device consists of a series combination of a bipolar transistor and an MOS p-type capacitor.[35]

During the scanning period the controlling potential changes from a high negative voltage to a value lower by an amount ΔV_G. The natural characteristic of the minority-carrier injection process is the time t_1 of transport under the influence of the voltage ΔV_G, and it can be made less than the time constant $R_L C_C$, where C_C is equal to the capacitance of the collector junction and the parasitic output capacitances. The voltage step created by the charge packet after a time t_1 is

$$\Delta U = \Delta V_G C_{ox}/C_C. \quad (15)$$

After completion of the injection process the voltage drops with a time constant $R_L C_C$. Usually $t_1 \approx 30$ nsec for the epitaxial layer and $R_L C_C = 0.3$ μsec. There is no direct electrical connection between the gate and the collector electrode.

The signal-to-noise ratio in such a system in inversely proportional to that part of the collector capacitance which is subject to the action of the potential drop in the thin epitaxial layer. To reduce this effect some doping is added to the collector, which in turn leads to a corresponding increase of the series-connected resistance. Therefore the output signal is stored in the collector capacitance and is read out only after the gate potential is discharged. Then the residual switching-noise signals cancel each other and after this the voltage on the capacitance C_C is in general not further subject to noise. The choice of thickness of the epitaxial layer is determined from the condition that, the thinner this layer, the more rapidly diffusion occurs and the less is the loss of charge in recombination during readout. However, with decrease of the thickness of the layer the photosensitivity decreases. Finally, the smaller the thickness of the epitaxial layer, the smaller is the cross modulation. For a large layer thickness, the photo-outflow current of the buried collectors is high. However, this current is small and is constant, in contrast to the signal, which has a pulsed structure.

Figure 17 shows the electrical readout circuit. Each element of the matrix is addressed directly by selection of the row of the silicon gate and then sensing of the corresponding column of the buried collector.[35]

An experimental sample of a three-electrode charge-injection device contains 24 rows and six columns with a step in the vertical direction of 100 μm. No cross modulation or image smearing in the vertical direction was observed. In the horizontal direction an anomalous effect due to the deep penetration of the thermal component of the light source was noted. The readout process in a three-electrode system, as in a photodiode matrix, can be carried out at the stage of photocharge storage, and here an intermediate memory is not required.

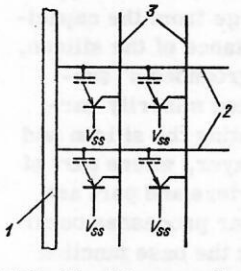

FIG. 17. Diagram of scanning system of CTD with three electrodes: 1—voltage-pulse generator, 2—horizontal buses, 3—vertical buses.

A system of this type has the following deficiencies: 1) reduction of the photosensitivity with increase of collector capacitance and difficulties in use of large matrices; 2) as in traditional designs of charge-transfer devices, large values of output capacitance of the collector increase the thermal noise and do not permit operation at low illumination levels; 3) the technology of preparation of such devices is more complicated than for photodiode matrices.

An advantage of the three-electrode system is that it permits a rate of change of frames up to 2×10^4 frames/sec to be achieved, in comparison with the television standard of 30 frames/sec.

It was already noted[20] in 1973 that CTD photodetectors will find extensive application in elementary-particle physics in photography under conditions of low illumination and under conditions where high geometrical accuracy of image reproduction is required. This question is discussed in detail in Secs. 8 and 9 of the present review.

6. MEMORY UNITS EMPLOYING CTDs

A one-dimensional shift register employing CTDs has the functional properties of a memory device capable of storing two-level and multilevel signals. As a result of the dark current, CTD memories can operate only in the dynamic mode. Therefore as a rule it is necessary to introduce a signal-regeneration system, and this in turn leads to distortion of the signal height.

The theoretical limit of the size of a CTD memory is determined by the probability of error as a result of inefficiency of charge transfer along the shift register.[1] If we introduce a parameter m related to the error probability P by the equation[1]

$$P = (0.6/m)\exp(-m^2/2), \quad (16)$$

then the maximum number of signal levels is

$$K_0 = (S/N)/2m \quad (17)$$

for $\varepsilon = 0$, where S/N is the signal-to-noise ratio. If $\varepsilon \neq 0$, then

$$K = (S/N)/2(m + n\varepsilon S/N). \quad (18)$$

CTD memory units are usually used as memory devices for binary information. The unit of measurement of the size of a memory is 1K = 1024 bits. To increase the size of a memory unit employing CTDs, individual CTD shift registers are combined into a more complicated system using various circuit arrangements: series, series-parallel-series (SPS), densely packed, and multiplex systems with one or

many phases. The more complicated the circuit organization, the higher the capacity of the memory.[22] In systems with series arrangement, the specific power dissipation does not depend on the length of the register. In the SPS arrangement the power dissipation increases with decrease of the length of an individual register. On the basis of the criterion of dissipated power, systems with a multiplexing organization are most advantageous. The greatest density of information recording is obtained in a multiphase SPS arrangement.

CTD memories carry out the following operations: writing, reading, and regeneration of information, storage of information without shift, and operation in the read-modify-record mode. In the write mode the initial data reach the place of storage of the information. Here the previous information is erased. In the read-modify-record mode the stored data are sent to the output, and in their place new data are recorded.

There are two classes of memory devices employing CTDs: with sequential sampling, capacity up to 16K, and clock frequency 10 MHz; with block sampling and capacity from 4 to 64 K at a frequency from 2 to 10 MHz; and also with arbitrary sampling up to 65K. Two stages of gates are used to separate the regions of storage and transfer of charge in a system with arbitrary sampling. In a system of double CTD elements it is possible to carry out nondestructive readout of information by means of a floating gate.[1]

The speed of operation of CTD memory devices is limited by the capacitance loading of the clock-pulse generator. In systems with block sampling the clock pulses go only to certain blocks, and the capacitance loading of the generator is small. All blocks are served by a single amplifier-register. The maximum sampling time of the first bit is 80 nsec, and on the average over the register it is 12 μsec. In comparison with memory devices employing MOS transistors, CTD systems occupy a factor of two less area: in CTD systems it is convenient to store analog information, and in them there are no contacts between the register elements.

The elements of a CTD memory with arbitrary sampling[36] have a construction similar to that of the element of a charge-injection device (Fig. 18). Writing of information in such an element is carried out by means of a diffusion bus with p^+ conductivity located inside a layer of silicon with n conductivity. Nondestructive readout is carried out by means of two electrodes, to which a difference voltage is supplied, by mutual interchange of potentials. When charge flows from one potential well to the other, a voltage pulse appears on the p^+ bus. Readout of information occurs simultaneously in all elements of a column or row.

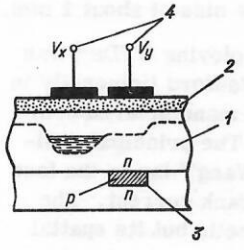

FIG. 18. Diagram of CTD memory cell: 1—semiconductor layer with n-type conductivity, 2—dielectric layer, 3—diffusion bus with p^+ conductivity, 4—electrodes of cell.

In order to increase the storage time of information in CTD memories, a metal-nitride-oxide-semiconductor (MNOS) structure is used,[64] which differs from an MOS structure in the presence of an additional layer of silicon nitride. Under the action of a high bias voltage supplied to the electrode, charge is expelled from the silicon substrate into the gap between the oxide and the nitride. The charge is captured in this layer and subsequently affects the threshold voltage of the MNOS structure. Under the action of a bias of the reverse polarity supplied to the electrode, the captured charge is removed from the gap between the oxide and the nitride. In contrast to traditional CTDs with the MOS structure, where the information is introduced in form of minority charge carriers, the agent of information introduction in an MOS structure is the electrical voltage pulse applied to the electrode. By means of an MNOS element of this type it is possible to prepare memory devices with arbitrary sampling and a storage time up to a year at room temperature.

The cost of CTD memory devices is 4–6 times less than that of magnetic drums or disks. An important advantage of CTD memory devices is the fact that a memory block can be realized in a single silicon crystal. It is expected[1] that in the near future multilevel CTD memory systems will be developed.

7. SPECTRAL TRANSFORMATIONS EMPLOYING CTDs IN REAL TIME

The most widely used form of transformation in the technology of spectral analysis is the discrete Fourier transform. It is possible to reduce a discrete folding or correlation to this form, and also to solve many problems of filtering and signal restoration. The decisive factor is the existence of fast algorithms for Fourier transformation by computer. Nevertheless digital algorithms for a discrete Fourier transformation have one important deficiency. Spectral transformation of a digital sequence cannot be started before quantization of the array of initial information is completed. In analog systems the situation is different. Here a Fourier transformation can be carried out in real time. For this it is sufficient to use a *chirp* algorithm for calculation of the discrete Fourier transform. The essence of the chirp algorithm is as follows.[1,55] If in a Fourier transform

$$F(\omega)=\sum_{x=0}^{N-1} f(x)\exp\left(\frac{2\pi i}{N}x\omega\right), \tag{19}$$

where $0\leqslant x\leqslant N-1$ and $0\leqslant\omega\leqslant N-1$, the initial function is specified in the form of an equidistant sequence of N readings and the quantity $2\times\omega$ is replaced by its algebraic equivalent

$$2x\omega=x^2+\omega^2-(\omega-x)^2, \tag{20}$$

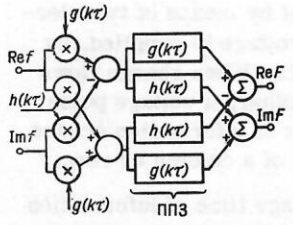

FIG. 19. Chirp algorithm for calculation of the discrete Fourier transform of a complex-valued function by means of CTD registers in real time.

then the Fourier transform $F(\omega)$ is written in the form

$$F(\omega)=\exp\left(-i\frac{\pi\omega^2}{N}\right)\sum_{x=0}^{N-1}f(x)\exp\left(-i\frac{\pi x^2}{N}\right)\exp\left(\frac{i\pi(\omega-x)^2}{N}\right). \quad (21)$$

The factor of the form $\exp(i\pi x^2/N)$ is called the chirp signal. The instantaneous frequency of such signals changes linearly with the coordinate x.

The structure of the expression (21) shows that finding the Fourier transform $F(\omega)$ of the initial function $f(x)$ reduces to a discrete folding and to two operations of multiplication by chirp signals. In Fig. 19 we have shown one possible realization of these operations by means of CTDs. The initial sequence of values of $f(x)$, $0\leqslant x\leqslant N-1$, is broken down into real and imaginary parts and each of these is fed to one of the two channels. In the first channel the analog operation of multiplication by the function $\cos\pi x^2$ is carried out, and in the quadrature channel—the operation of multiplication by the function $\sin\pi x^2$. The cross sum and difference components are fed to correlators and delay lines constructed of CTDs. Altogether there are four channels with cross connections at the output. Each of the output sequences goes to the direct and the quadrature channels. The device has two outputs. At the first of these the real component $F_{\mathrm{Re}}(\omega)$ appears, and at the second—the imaginary component $F_{\mathrm{Im}}(\omega)$. If it is required to find the spectrum of signal strength, then the chirp-algorithm scheme is realized more simply (Fig. 20). The weight functions of the correlator, which is based on CTDs, are equal to the values of the readings of the direct and quadrature chirp signals:

$$\left.\begin{aligned} g(k\tau)&=\cos[\xi(k\tau)^2];\\ h(k\tau)&=\sin[\xi(k\tau)^2],\quad -T_d/2<k\tau<T_d/2,\end{aligned}\right\} \quad (22)$$

where ξ is a coefficient specifying the scale of the chirp signal; T_d is the duration of the pulse response, and τ is the clock period. The time T_d is limited on the high side by processes of charge-carrier thermal production in the CTD cells and amounts to 1–10 sec.

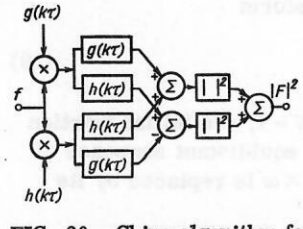

FIG. 20. Chirp algorithm for calculation of signal-strength spectum by means of CTD registers in real time.

The corresponding limiting resolution in frequency is 0.1–1 Hz.

The accuracy with which CTDs carry out a discrete Fourier transformation by means of a correlation chirp algorithm is substantially poorer than the accuracy of calculation of a discrete Fourier transform by computer. For example, the uncertainty in the amplitude due to technical factors in the preparation of the weighting masks of the CTDs is at least $1:10^3$, which is equivalent to no more than ten binary digits. CTD chirp correlators described in the literature contain a chain of 500 elements, operate at clock frequency 20 kHz, and calculate a spectrum with a resolution 1:500 at a frequency of 40 Hz in 25 msec. The dynamic range of CTD correlators is $10^4:1$. Estimates show that it is possible to construct CTD correlators with a number of cells up to 10^3 and with clock frequency up to 20 MHz. The universal parameter characterizing the information-transmission capacity of an information-processing system and its speed of operation is the product of the duration of the processing cycle and the frequency bandwidth. For CTDs this quantity is limited on the high side to a value of approximately 10^5.

8. STREAMER CHAMBER WITH CTDs

Tracks formed in a streamer chamber are usually photographed by means of high-aperture optical systems.[38] Recently researchers have begun to record the information holographically,[47] which provides a higher spatial resolution.[39] A common deficiency of these two methods is the fact that the analysis of a large number of track photographs occupies an extended period of time. In order to accelerate this process physicists have begun to go over to filmless systems of recording track information.[40] In particular, Vidicon systems and systems with image amplifiers[41] are used to record tracks in streamer chambers.

The operation of readout of information from a Vidicon screen is slow, and this is the weakest point of the electron-optical systems of information readout from streamer chambers. An advantage of CTDs is that they are self-scanning systems, they have rapid action, and geometrical distortions are completely absent in them. Finally, the principle of action of CTDs permits one to combine the filtering and compression of the information with the track readout process in streamer chambers. We recall that a streamer formed under the action of an electric-field pulse lasts about 10^{-8} sec and has an effective size of about 1 mm.

The first streamer chamber employing CTDs[42] was prepared by Villa and Wang[42] at Stanford University in 1977. They used type 202A CTDs manufactured commercially by firms in the USA.[43] The principal difficulties encountered by Villa and Wang[42] lay in the fact that type 202A CTDs have a high dark current. The dark current varies from cell to cell, but its spatial pattern is stable in time. The random noise level is about 10^{-2} of the average level of dark current for a clock frequency 2 MHz and room temperature.

An image of the streamer tracks appearing in the two-meter streamer chamber at the Stanford laboratory[43] was formed by means of an objective with a focal length 25 mm and an aperture 1:2 in a matrix of 100×100 202A CTDs with a cell size 14×30 μm^2. The linear geometrical reduction accomplished by the optics was 1:160.

Readout of the image from the matrix was carried out at a clock-pulse frequency 4.5 MHz. If the amplitude of the signal coming from the output of the chain of CTD cells exceeded a specified threshold, then the clock-pulse generator stopped for a time of 25 μ sec. The X and Y coordinates of the cell and the height of the pulse in the cell, quantized in an ADC system, were stored in a memory block. As the result of misadjustments in the ADC system, information on the pulse heights did not arrive at the memory block and was observed on a cathode-ray-tube screen.

At the same time the streamer tracks were photographed by an ordinary camera on photographic film. It was observed that with a low discrimination level in a certain part of the matrix a bright region of illumination appears from the dark current. The width of the tracks obtained by means of CTDs amounts to 1/2 of the cell width or 7.5 μm.

The data obtained by Villa and Wang in their preliminary experiments must be considered as encouraging. These authors propose in the future to use type 211 CTDs, whose matrix consists of 244×190 cells of size 18×14 μm^2, and the clock frequency will be 7 MHz. This permits the geometrical reduction coefficient to be decreased and permits an accuracy comparable with that given by photographic emulsion to be achieved. In addition, the 211 CTD has a higher sensitivity and the dark-current pattern can be reduced to the required level by cooling of the CTD matrix to a temperature −20°C.

Open questions which remain are the dynamic range of CTDs and their potential for withstanding overexposure for particles traveling at a small angle (< 30°) to the electric-field vector. The tracks of such particles have a spark mode and their brightness is 10^3 times greater than for the streamer mode. The antihalo layer used in photographic emulsion reduces the effect of excessive exposure. The brightness of a streamer track in a CTD matrix, estimated by Villa and Wang, is about 1:200 of the CTD saturation level. Therefore the excess exposure coefficient of CTDs is 10–1, and this will be quite sufficient to illuminate completely the entire chain of CTD cells.

An experimental comparison of the parameters of CTDs with a photographic emulsion was carried out by Wallick *et al.*[44] for an exposure time of about 0.25 μsec. The sensitivity of a type 202 CTD was determined for images in neon light, and this was compared with the corresponding parameters of Kodak SO-143 emulsion, which is considered to be the best for use in streamer chambers. It was shown that the light sensitivity of the CTD-202 matrix cooled to −10°C is an order of magnitude greater than the sensitivity of the best Kodak SO-143 film. It was also observed that cooling CTDs below −15°C is undesirable, since in this region the output-circuit noise is dominant. A CTD-201 cooled to −50°C was used successfully in astronomical photodetectors. A thermoelectric refrigerator was used to cool the CTD matrix. The measured dependence of the average dark current on the temperature is described by an exponential. It is desirable to carry out the cooling to the temperature at which the dark signal becomes substantially less than the useful signal.

The high sensitivity of a CTD matrix cooled to −10°C permits reduction of the length of the high-voltage pulse which produces streamers along the charged-particle path. The shorter streamers increase the accuracy of the measurements and reduce the intensity of parasitic illumination of the chamber volume.

The image obtained from the CTD matrix has a quantized form and can be transferred to the screen of the cathode-ray tube of a dialogue system for subsequent processing by means of a light pencil. This information can be processed on-line with the experiment. The advantages of filmless systems of information readout from track chambers are realized most clearly in CTD systems.

9. TOPOLOGICAL TRANSFORMATIONS IN READOUT OF TRACK IMAGES BY MEANS OF CTDs

The volume of information coming from a streamer chamber is relatively large, and only a small fraction of the image elements contain signal charges. For example, no more than 5×10^4 cells turn out to be illuminated in a total matrix of 10^6 cells. An overwhelming fraction of the cells turn out to be either empty or to contain a bias-charge signal. Here each streamer of a track has a high spatial correlation with the neighboring streamer. The streamers form simple geometrical lines: straight lines, arcs of circles, or curves of third order—and they all originate from a pointlike region where the nuclear event occurred. This means that the number of independent components of information in photographs in a streamer chamber is extremely small. It is desirable to find these independent components directly in the process of readout of information from the CTD matrix.

Kozhevnikova and Soroko[45] have developed an algorithm for scanning straight-line tracks by means of Walsh masks. The essence of this algorithm is the fact that in the scanning of straight-line tracks a rapid search is carried out for invariant components of the discrete Walsh transform, omitting the operation of determining the complete set of components of the two-dimensional Walsh transform. In constructing the algorithm for searching for invariant components of the two-dimensional Walsh transform of a straight-line track, these authors utilized the fact that the Walsh-transform components invariant to shift are in the last row and in the last column of the transform matrix of the track. The basis of the algorithm is an iterative process of scanning the edge elements of the

transform matrix with successive breakdown into two equal parts of the corresponding set of components of the Walsh transform. This set is either the initial set or it arises after a previous scanning cycle.

There is a sequence of modified Walsh masks which permit direct determination of the value of sums calculated at different stages of information readout. The scanning process is carried out by means of modified Walsh masks, omitting the operation of finding all components of the Walsh transform.

The algorithm described in Ref. 45 for searching for invariant components of a Walsh transform of straight-line tracks can be realized by means of charge-injection devices, making use in particular of the method of nondestructive readout[13] or sequential injection of signal charges into the horizontal buses.

However, this algorithm has several deficiencies, which are mainly due to the fact that the search is not topological and in all steps except the last it does not operate with the complete track image.

A principle of action of an algorithm for topological analysis of particle tracks has been developed by Soroko[46] for the case of a straight-line track. The scanning process is carried out by means of a CTD matrix with the important distinction that the clock pulses are fed not to all rows of the CTD matrix, but selectively. In the case of straight-line tracks the number of clock pulses transmitted to each row of the CTD matrix is changed according to a stepwise linear law. Therefore straight-line tracks are rotated with respect to the CTD matrix as an integral whole without destroying their topological characteristics. This rotation is carried on until the track occupies a vertical position. On the reverse side of the CTD matrix or charge-injection device are located vertical buses which have an electrical capacitive connection to each of the columns of the CTD matrix. At the time when a track occupies a vertical position, the signal on the corresponding vertical bus will reach its maximum value. The coordinate of the vertical bus on which the maximum signal is formed is equal to the coordinate of exit of the track into the upper part of the frame. The slope angle of the track in its initial position before the start of the scanning is determined by the number of clock periods of operation of the clock-pulse generator. The data on the coordinate of entry of the track into the frame and its slope angle are quantized and are directed to a memory block. To further accelerate the scanning of track images, the entire frame is broken down into small sections of size 8×8 or 16×16 and the topological operations of scanning are carried out simultaneously in all sections. At a clock-pulse repetition frequency of about 50 MHz the total scanning time for a frame is about 0.5 μsec. If there are several tracks with different entry coordinates and different slope angles in a frame, maxima in the comb of vertical buses arise as many times as there are tracks in the frame.

In Fig. 21 we have shown eight column vectors which specify a sequence of shifts by one step to the right.

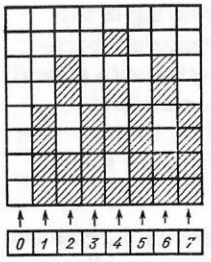

FIG. 21. Set of eight column vectors which specify the algorithm for transmission of clock pulses to the horizontal registers of a CTD matrix.

The dark fields signify that in this register the picture is shifted by one step to the right, and the white fields correspond to those registers to which clock pulses are not fed. In the lower row we have indicated the numbers of the cycles. The zeroth cycle corresponds to the initial track pattern in the frame. It is not without interest to note that the matrix in Fig. 21, which characterizes a set of shifts by one step to the right, coincides with the matrix of trigger voltages in J–K triggers which form part of the generators of discrete Walsh functions.[48]

CONCLUSION

Semiconductor microminiature technology, which forms the basis for charge-transfer devices, is developing at a rapid rate. The number of fields of science and technology in which CTDs are finding application appropriate to their physical and technical characteristics is constantly being extended. We give several typical illustrations of this process.

A CTD matrix as a detector of infrared radiation has been successfully used in astronomy in the Arizona telescope, $D = 155$ cm, and the Polomar telescope, $D = 510$ cm. The space ship which was sent to the planet Jupiter was supplied with a television camera in the form of a CTD matrix of size 800×800 elements. The absence of any geometrical distortions in this system of scanning permits determination of the coordinates of objects with high accuracy.

New models of delay lines employing CTDs have been prepared with 4096 elements and delay time 0.2 sec. Transversal CTD filters and real-time Fourier transformation systems with 512 elements have been prepared. It is expected that the accuracy of calculations in these systems will be higher than in digital computers.

CTD memory devices with large capacity and arbitrary sampling are being intensively developed. It is expected that by 1980 compact CTD memory blocks of capacity 128K and 256K will be produced.

[1]C. Sèquin and M. Tompsett, Charge Transfer Devices, Academic Press, New York, 1975 (Supplement 8, Advances in Electronics and Electron Physics). Rus.. transl., Pribory s perenosom zaryada, Mir, Moscow, 1978.
[2]Yu. R. Nosov and V. A. Shilin, Poluprovodnikovye pribory s

zaryadovoĭ svyaz'yu (Semiconductor Charge-Coupled Devices), Soviet Radio, Moscow, 1976.
[3]D. F. Barbe, Proc. IEEE **63**, 38 (1975). Russ. transl., TIIÉR **63**, No. 1, 45 (1975).
[4]W. S. Boyle and G. E. Smith, Bell Syst. Tech. J. **49**, 587 (1970).
[5]A. J. Steckl *et al.*, Proc. IEEE **63**, 67 (1975). Russ. transl., TIIÉR **63**, No. 1, 79 (1975).
[6]C. N. Berglund *et al.*, Appl. Phys. Lett. **20**, 413 (1972).
[7]R. D. Melen and J. D. Meindl, IEEE J. **SC-7**, 92 (1972).
[8]R. H. Walden *et al.*, Bell Syst. Tech. J. **51**, 1635 (1972).
[9]V. A. Gergel', Mikroélektronika (Microelectronics) **2**, No. 5, 415 (1973).
[10]L. Boonstra and F. L. Sangster, Electronics **45**, 64 (1972).
[11]D. F. Barbe, Electron. Lett. **8**, 207 (1972).
[12]F. Villa and L. C. Wang, Nucl. Instrum. Methods **144**, 533 (1977).
[13]H. K. Burke and G. J. Michon, IEEE J. **SC-11**, 21 (1976).
[14]C. H. Sequin *et al.*, IEEE J. **SC-11**, 115 (1976).
[15]D. D. Wen and P. J. Salsbury, ISCCC, Philadelphia, Digest of Techn. Papers, 1973, p. 154.
[16]D. D. Wen, IEEE J. **SC-9**, 410 (1974).
[17]D. R. Collins *et al.*, Electron. Lett. **8**, 328 (1972).
[18]V. Zhalud and V. N. Kuleshov, in: Shumy v poluprovodnikovykh ustroĭstvakh (Noise in Semiconductor Devices), Soviet Radio, Moscow Publishing House of Technical Literature, Prague, 1977.
[19]D. H. Seib, IEEE Trans. **ED-21**, 210 (1974).
[20]B. A. Kondratskiĭ, L. A. Logunov, and V. A. Shilin, Zarubezhnaya élektronnaya tekhnika (Foreign Electronics Technology), No. 15, 16 (1974).
[21]B. M. Khotyanov and V. A. Shilin, Zarubezhnaya élektronnaya tekhnika (Foreign Electronics Technology), No. 9, 10 (1975).
[22]B. M. Khotyanov and V. A. Shilin, Zarubezhnaya élektronnaya tekhnika (Foreign Electronics Technology), No. 23, 24 (1976); No. 1, 2 (1977).
[23]A. V. Veto *et al.*, in: Mikroélektronika (Microelectronics), No. 8, Soviet Radio, Moscow, 1975, p. 50.
[24]P. E. Kandyba *et al.*, in: Mikroélektronika (Microelectronics), No. 7, Soviet Radio, Moscow, 1974, p. 55.
[25]Yu. R. Nosov and V. A. Shilin, Zarubezhnaya élektronnaya tekhnika (Foreign Electronics Technology), No. 13 (1974).
[26]M. F. Tompsett and E. F. Zimany, IEEE J. **SC-8**, 151 (1973).
[27]R. C. Tozer and G. S. Hobson, Electron. Lett. **12**, 444 (1976).
[28]J. D. Meindl, in: Acoustic Imaging, Ed. G. Wade, Plenum Publ. Co., 1976, p. 127.
[29]R. D. Baertsch *et al.*, IEEE J. **SC-11**, 65 (1976).
[30]R. W. Brodersen *et al.*, IEEE J. **SC-11**, 75 (1976).
[31]W. J. Butler *et al.*, Electron. Lett. **8**, 543 (1972).
[32]D. F. Barbe, IEEE J. **SC-11**, 109 (1976).
[33]A. V. Veto *et al.*, in: Mikroélektronika i poluprovodnikovye pribory (Microelectronics and Semiconductor Devices), No. 2, Soviet Radio, Moscow, 1977, p. 216.
[34]D. M. Brown *et al.*, IEEE J. **SC-11** 128 (1976).
[35]P. G. Jespers and J. M. Millet, IEEE J. **SC-11**, 133 (1976).
[36]R. T. Baker, Electronics **48** 138 (1975).
[37]J. B. G. Roberts, Electron. Lett. **12**, 452 (1976); IEEE J. **SC-11**, 100 (1976).
[38]V. V. Ermolaev *et al.*, Communication R10-9949, JINR, Dubna, 1976.
[39]V. S. Kozlov *et al.*, Preprint No. 262, Leningrad Institute of Nuclear Physics, 1976.
[40]Yu. V. Zanevskiĭ, Fiz. Elem. Chastits At. Yadra **8**, 631 (1977) [Sov. J. Part. Nucl. **8**, 259 (1977)].
[41]Yu. Beger *et al.*, Communication R13-10219, JINR, Dubna, 1976.
[42]F. Villa and L. C. Wang, SLAC-PUB-1890, 1977.
[43]W. Wallick and R. Kenyon, Reprint DN-28, University of Washington Seattle, 1976.
[44]W. O. Wallick *et al.*, Nucl. Instrum. Methods **146**, 403 (1977).
[45]S. O. Kozhevnikova and L. M. Soroko, Communication R10-7757, JINR, Dubna, 1974.
[46]L. M. Soroko, Communication R10-11515, JINR, Dubna, 1978.
[47]L. M. Soroko, Fiz. Elem. Chastits At. Yadra **3**, 688 (1972) [Sov. J. Part. Nucl. **3**, 352 (1972)].
[48]P. M. Besslich, IEEE Trans. **EMC-15**, 177 (1973).
[49]M. M. Krymko *et al.*, in: Mikroélektronika i poluprovodnikovye pribory (Microelectronics and Semiconductor Devices), No. 2. Soviet Radio, Moscow, 1977, p. 211.
[50]V. P. Popov *et al.*, in: Mikroélektronika i poluprovodnikovye pribory (Microelectronics and Semiconductor Devices), No. 2, Soviet Radio, Moscow, 1977, p. 243.
[51]E. V. Vlasenko *et al.*, in: Mikroélektronika i poluprovodnikovye pribory (Microelectronics and Semiconductor Devices), No. 2, Soviet Radio, Moscow, 1977, p. 223.
[52]I. E. Carnes and W. F. Kosonocky, Appl. Phys. Lett. **20**, 261 (1972); RCA Review **33**, 327 (1972).
[53]M. A. Copeland *et al.*, IEEE J. **SC-11**, 84 (1976).
[54]L. F. Lind and W. S. Matheson, Electron. Lett. **12**, 343 (1976).
[55]Semiannual Technical Report USC IPI-660, 200 (1976).
[56]W. J. Butler *et al.*, IEEE J. **SC-11**, 93 (1976).
[57]S. Chen, IEEE J. **SC-11**, 93 (1976).
[58]K. R. Hense and T. W. Collins, IEEE J. **SC-11**, 197 (1976).
[59]A. M. Mohsen *et al.*, IEEE J. **SC-11**, 49 (1976).
[60]W. E. Tchon *et al.*, IEEE J. **SC-11**, 25 (1976).
[61]L. M. Terman and L. G. Heller, IEEE J. **SC-11**, 4 (1976).
[62]M. F. Tompsett *et al.*, IEEE Trans. **ED-18**, 992 (1971).
[63]G. F. Vanstone, Electron. Lett. **8**, 13 (1972).
[64]J. T. Wallmark and J. H. Scott, RCA Review **30**, 335 (1969).
[65]V. A. Zimoglyad *et al.*, in: Élektronnaya tekhnika. Ser. 3. Mikroélektronika (Electronic Technology. Series 3. Microelectronics), No. 2, Soviet Radio, Moscow, 1973.
[66]H. J. Whitehouse, IEEE J. **SC-11**, 64 (1976).
[67]A. Rose, editor, Vision, Human and Electronic. (Optical Physics and Engineering Series), Plenum Publ. Corp., 1973. Russ. transl., Mir, Moscow, 1977.
[68]V. Yu. Berezin *et al.*, Tekh. Kino Telev. (Technology of Motion Pictures and Television), No. 6, 54 (1977).

Translated by Clark S. Robinson